

NUMERICAL SIMULATIONS OF FLOW DUE TO DROP IMPACT ON A POROUS SUBSTRATE USING A PERMEABLE WALL MODEL

Edin Berberović
University of Zenica, Polytechnic Faculty
Fakultetska 1, 72000 Zenica
Bosnia and Herzegovina

ABSTRACT

The computational model for the isothermal free-surface flow pertinent to drop impact and spreading on the porous substrate using a permeable wall model is formulated. The model uses the interface capturing methodology implemented in the open-source software OpenFOAM® based on the volume-of-fluid (VOF) method in the framework of Computational Fluid Dynamics (CFD) to compute the external flow of the spreading liquid upon the drop impact, and the effects of the porous substrate are accounted for by introducing a permeable wall boundary condition. The capability of the model is verified by comparing the numerical results with the available experimental data.

Keywords: numerical simulation, CFD, free-surface flow

1. INTRODUCTION

The interfacial flow associate with impacts of liquid drops onto porous surfaces is a type of two-phase flow which is common in everyday life and in engineering. Examples of application include ink-jet printing, manufacturing of composite materials or even in medicine for needle-free drug delivery by penetrating liquid medication into human skin. The wetting characteristics of the liquid/porous surface are of great importance for a successful application of such technologies. The flow consists of liquid spreading over and absorption into the porous substrate, depending on the wettability, porosity and permeability of the porous substrate. The complexity of the flow makes experimental access difficult and permits only simplified analytical solutions for the flow dynamics. The flow is characterized by different time scales, one for the liquid spreading and the other for the penetration [1], which is several orders of magnitude larger. In the present study the numerical procedure for interface capturing similar to the one in [2] is adopted to compute drop impact on a porous surface. The computational model originating from the volume of fluid (VOF) method [2,3] is revised to compute only the liquid spreading in the external flow, and the effects of the porous substrate are accounted for by an appropriate permeable wall boundary condition. The capability of the numerical model is verified by comparing the results obtained computationally with the existing experimental data [4].

2. COMPUTATIONAL MODEL

In the studies of the flow through porous media the attention was given to single-phase flows and estimations of permeability and porosity. Theoretical expressions are obtained for simplified unidirectional flow along long cylinders, and the data is presented in the dimensionless form $K / R_p^2 = f(\phi)$, where K is permeability of the fibrous material, R_p is the characteristic dimension (radius) of pores, and $\phi = 1 - \varepsilon$ is the solid volume fraction with the porosity calculates as $\varepsilon = V_p / V$.

An overview of the estimations of $f(\phi)$ is provided in Jackson and James [5], and a theoretical model for the permeability of an orthogonal pattern fibrous web is presented in [6]. Under assumption of a very slow liquid flow in the fibrous porous material it can be approximated by the steady Stokes flow, the solution of which and the corresponding liquid mean velocity for the case of cylindrical pores are

$$U = \frac{1}{4\mu} \frac{\partial p}{\partial z} (r^2 - R^2), \quad \langle U \rangle = -\frac{R^2}{8\mu} \frac{\partial p}{\partial z}. \quad \dots (1)$$

The external flow is solved using the interface capturing model [7] consisting of the governing transport equations are the conservation of mass, phase fraction and momentum

$$\nabla \cdot \mathbf{U} = 0, \quad \dots (2)$$

$$\frac{\partial \gamma}{\partial t} + \nabla \cdot (\mathbf{U}\gamma) + \nabla \cdot [\mathbf{U}_c \gamma (1 - \gamma)] = 0, \quad \dots (3)$$

$$\frac{\partial (\rho \mathbf{U})}{\partial t} + \frac{1}{\varepsilon} \nabla \cdot (\rho \mathbf{U} \mathbf{U}) = -\nabla p_d - \varepsilon \mathbf{g} \cdot \mathbf{x} \nabla \rho + \nabla \cdot \boldsymbol{\tau} + \varepsilon \sigma \kappa \nabla \gamma, \dots (4)$$

where all the variables are defined in [7]. The model represents the one-fluid approach, treating fluids as a homogeneous mixture of gas and liquid, the properties of which determined as weighted averages based on the phase fraction distribution. Surface tension force is accounted for by the Continuum Surface Force model [8]. The numerical simulations were carried out using OpenFOAM® [9]. The flow is solved in an iterative solution procedure with fluid properties being updated after each time step determined by the phase fraction distribution. The solution procedure incorporates a cell-centered finite volume approximation where special care is taken for the spatial convective derivatives which are integrated over cell face surfaces using flux limiters. The pressure is coupled with velocity by the Pressure Implicit with Splitting of Operators (PISO) algorithm. The computational domain for the permeable wall model, shown in Fig. 1, is a two-dimensional axisymmetric slice including only the external region with the permeable wall boundary condition at the porous surface.

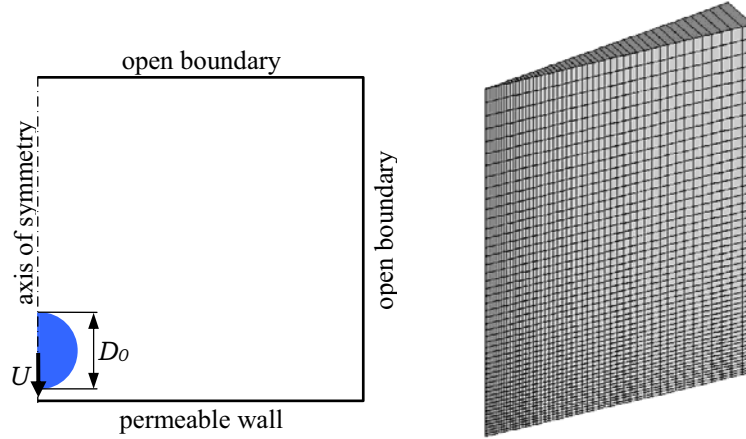


Figure 1. Initial case configuration (left) and computational mesh (right).

The mesh is graded, with dimensions in the vertical plane of $4D_0 \times 6D_0$ based on the droplet initial diameter with the total of 40000 cells. The initialization includes prescribing the phase fraction distribution corresponding to the shape of one drop and setting the initial impact velocity. The boundary conditions include open boundaries at the top and to the right side with the prescribed total pressure and a combination of inlet and outlet conditions for velocity. The permeable wall boundary condition at the impacting surface is formulated by expressing the normal-to-the-surface velocity component from Eq. (1) and making use of the fact that the velocity is continuous in the thin region in the vicinity of the plane of the porous surface begins, as shown in Fig. 2, yielding

$$U|_{\perp} = -\frac{K_{down}}{\mu_{down}} \nabla p_{down} \Big|_{\perp} = -\frac{K_{up}}{\mu_{up}} \nabla p_{up} \Big|_{\perp}. \quad \dots (6)$$

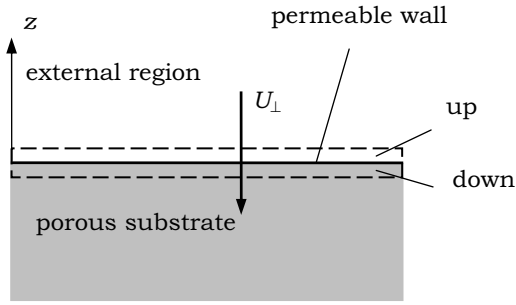


Figure 2. The permeable wall.

Table 1. Properties of the liquid and porous medium.

n-heptane/ceramic	
density ρ , kg/m ³	667.5
viscosity μ , Ns/m ²	$4.05 \cdot 10^{-4}$
surface tension σ , N/m	$2.01 \cdot 10^{-2}$
porosity ε , -	0.25
permeability K , m ²	$1.04 \cdot 10^{-12}$
pore radius R_p , μm	2.88
Weber number, -	43
Reynolds number, -	2300

Most studies of drop impact on fibrous media do not provide exact values for the permeability or pore radius. The porous medium is commonly characterized by the porosity, or the area density and the thickness, which is insufficient for the simulation [10,11,12]. The assessment of the computational models is performed by comparison of the numerical results with the experimental data for drop impact on the porous substrate [4] where the liquid used is n-heptane (C7H16) with properties listen in Table 1, the initial drop velocity of $U_0 = 0.93$ m/s and the drop diameter of $D_0 = 1.5$ mm.

3. RESULTS

To assess the predictive potential of the model, the spreading ratio, the lamella height at the symmetry axis, the lamella volume above and mean velocity at the porous surface were computed and compared to the experimental data in [4]. The results are shown in Figs. 3 to 6.

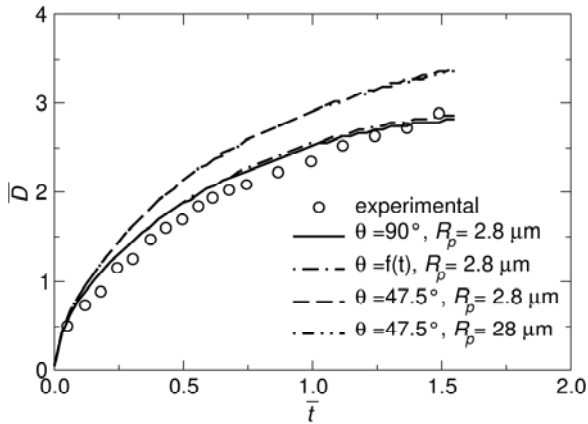


Figure 3. Drop spreading ratio

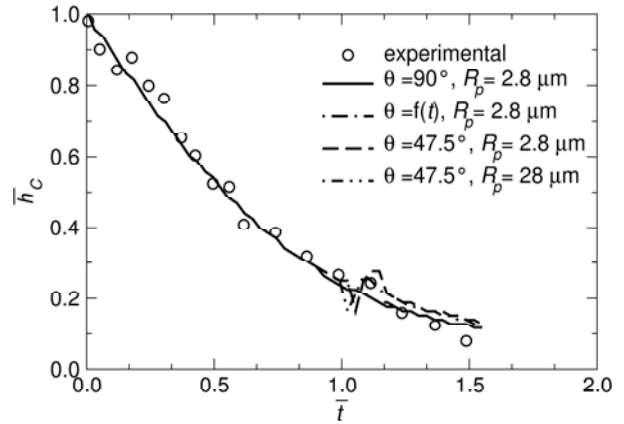


Figure 4. Lamella height at the symmetry axis

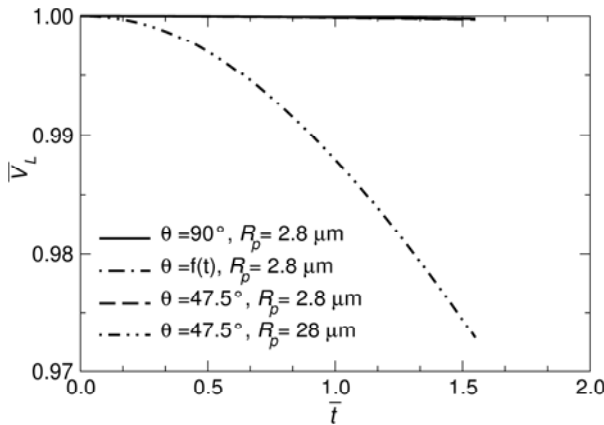


Figure 5. Lamella volume above the surface

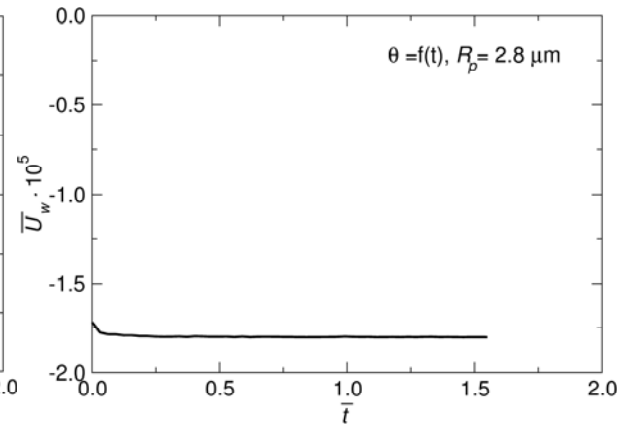


Figure 6. Mean velocity at the porous surface

Fig. 3 and Fig. 4 show the comparison of the computed spreading ratio and the lamella height at the axis of symmetry with the existing experimental results (normalized by the drop initial diameter and volume), and Fig. 5 and Fig.6 show the computed residual liquid volume and the mean velocity at the porous surface (normalized by the drop initial volume and impact velocity). Different contact angles were used in simulations. The results show a closer agreement with the experimental results compared to the combined model used in [2]. The disagreement of the spreading ratio is higher at lower contact angles. The permeability has negligible effects on the results in the initial inertia dominated flow due to larger time scale for the absorption. The small peak in the results for the lamella height at time $\bar{t} \approx 1.1$ is caused by the entrapped air bubble in the region of impact, which moves upwards and escapes through the free surface of the lamella. The residual liquid volume is non-linear in time for the higher permeability, whereas at lower permeability the volume is linear in time. Due to the constant wall pressure gradient, the mean velocity remains constant in accordance with Eq. (1).

4. CONCLUSIONS

The numerical model for a free-surface flow pertinent to drop impact on a porous surface is presented, incorporating the free-surface capturing based on the volume-of-fluid method with the permeable wall boundary condition at the impacting surface. The capability of the model is assessed by comparing the numerical results with the existing experimental data. The results for the drop spreading ratio and the lamella height show a good agreement with the experiments. The numerical solution procedure shows good predictive capabilities by reproducing correctly the characteristics of the studied flow.

5. ACKNOWLEDGEMENTS

The author would like to thank the Department for Fluid Mechanics and Aerodynamics at the Technical University of Darmstadt (SLA) for providing the research facilities to conduct the study and to the German Academic Exchange Service (DAAD) for the financial support.

6. REFERENCES

- [1] Golpaygan A., Hsu N., Ashgriz N.: Numerical investigation of impact and penetration of a droplet onto a porous substrate, *Journal of Porous Media*, Vol. 11, pp. 323-341, 2008.
- [2] Berberovic E.: Computational modeling of free-surface flow pertinent to droplet impact on a porous substrate, *Proceedings of the 18th International Research/Expert Conference "Trends in the Development of Machinery and Associated Technology" TMT 2014, Hungary*, pp. 209-212, 2014.
- [3] Hirt C.W., Nichols B.D.: Volume of fluid (VOF) method for the dynamics of free boundaries, *Journal of Computational Physics*, Vol. 39, pp. 201-225, 1981.
- [4] Chandra S., Avedisian C.T.: Observations of droplet impingement on a ceramic porous surface, *International Journal of Heat and Mass Transfer*, Vol. 35, pp. 2377-2388, 1992.
- [5] Jackson G.W., James D.F.: The permeability of fibrous porous media, *The Canadian Journal of Chemical Engineering*, Vol. 64, pp. 364-374, 1986.
- [6] Koponen A., Kandhai D., Hellen E., Alava M., Hoekstra A., Kataja M., Niskanen K., Slood P., Timonen J.: Permeability of three-dimensional random fiber webs, *Physical Review Letters*, Vol. 80, pp. 716, 1998.
- [7] Berberović E., van Hinsberg N.P., Jakirlić S., Roisman I.V., Tropea C.: Drop impact onto a liquid layer of finite thickness: Dynamics of the cavity evolution, *Physical Review E*, Vol. 79, pp. 036306, 2009.
- [8] Brackbill J.U., Kothe D.B., Zemach C.: A continuum method for modeling surface tension, *Journal of Computational Physics*, Vol. 100, pp. 335-354, 1992.
- [9] Jasak H., *OpenFOAM: Open source CFD in research and industry*, *International Journal of Naval Architecture and Ocean Engineering*, Vol. 1, pp. 89-94, 2009.
- [10] Arora D., Deshpande A.P., Chakravarthy S.R., Experimental investigation of fluid drop spreading on heterogeneous and anisotropic porous media, *Journal of Colloid and Interface Science*, Vol. 293, pp. 496-499, 2006.
- [11] Kumar S.M., Deshpande, A.P., Dynamics of drop spreading on fibrous porous media, *Colloids and Surfaces A: Physicochemical Engineering Aspects*, Vol. 277, pp. 157-163, 2006.
- [12] Clarke A., Blake T.D., Carruthers K., Woodward A., Spreading and imbibition of liquid droplets on porous surfaces, *Langmuir*, Vol. 18, pp. 2980-2984, 2002.